Acta Cryst. (1983). A**39**, 377–387

Generalized Relations Between *d*-Orbital Occupancies of Transition-Metal Atoms and Electron-Density Multipole Population Parameters from X-ray Diffraction Data*

BY A. HOLLADAY, P. LEUNG AND P. COPPENS†

Department of Chemistry, State University of New York at Buffalo, Buffalo, New York 14214, *USA*

(*Received* 15 *July* 1982; *accepted* 18 *November* 1982)

Abstract

Generalized relations relating multipole population parameters to *d*-orbital occupancies of transition-metal atoms are presented. The relations are cast in the form of a 15 × 15 matrix which reduces to smaller size for site symmetries higher than $\bar{1}$. The matrix takes into account differences in normalization of density functions and atomic orbitals. The expressions are applied to diffraction data on $Cr(CO)_6$, $Mn_2(CO)_{10}$, $Co_2(CO)_8$, $Co_3(CO)_9CH$, $Co(NH_3)_6Cr(CN)_6$ and $Co(NH_3)_6$-$Co(CN)_6$. In all cases crystal-field destabilized orbitals are depopulated relative to stabilized orbitals. Results are in almost quantitative agreement with theoretical populations; small remaining discrepancies are to be analyzed further for their possible significance. Occupancy of e_g' orbitals in the last two compounds indicates a degree of covalency of the metal–ligand interaction in these low-spin complexes which is larger for the cyano ligand than for the ammonia molecule in agreement with generally accepted conclusions based on spectroscopic data. Very little difference is observed between the relative orbital occupancies of the $Cr(CN)_6^{3-}$ and $Cr(CO)_6$ species.

Introduction

The number of experimental electron-density studies on crystals containing transition-metal atoms has increased considerably in recent years. Whereas metals such as iron, vanadium and aluminum were the subject of early studies (Weiss & Mazzone, 1982), much recent work has concentrated on more complicated coordination complexes, metal cluster compounds, minerals and metalloorganic substances (*e.g.* Iwata & Saito, 1973; Rees & Coppens, 1973; Rees & Mitschler, 1976; Benard, Coppens, DeLucia & Stevens, 1980; Wang & Coppens, 1976; Downs, Hill, Newton, Tossell & Gibbs, 1982).

Though deformation density maps have proven to be unusually informative for a qualitative assessment of the nature of chemical bonding, there is an obvious need for a quantitative evaluation of the results. For example, methods have been developed to derive both 'inner' moments [such as the electric field gradient at the nucleus (Stewart, 1972, 1977)] and 'outer' moments [such as a net charge or a molecular dipole moment (Moss, Hansen & Coppens, 1980)] from the X-ray diffraction data.

In the case of transition-metal atoms *d*-orbital occupancies have been derived from least-squares multipole population coefficients, using point-group-specific relations, which are valid under the assumption that the *d* orbitals can be represented by single Slater-type orbitals and that the overlap between metal atom and ligand orbitals is small (Stevens & Coppens, 1979).

In this paper we describe a generalized relation, valid in point group $\bar{1}$ (the *d* orbitals being even functions), from which point-group-specific expressions can be readily derived. The relations are applied to a number of data sets and results are compared with available theoretical values.

Description of the expressions

The relationship between *d*-orbital occupancies and multipole population parameters is derived from the equivalence of two alternative descriptions of the atomic electron density.

(*a*) *The electron density in terms of atomic orbitals*

The *d*-electron density may be expressed in terms of the atomic orbitals d_l, each consisting of a common radial part $R(r)$ multiplied by an angular function $y_{lm\pm}$, which is a real spherical harmonic. The *d*-electron density can then be written as

$$\rho_d = \sum_{l=1}^{5} P_l d_l^2 + \sum_{l=1}^{5} \sum_{j>l}^{5} P_{lj} d_l d_j \qquad (1)$$

with

$$d_l = R(r) y_{lm\pm}.$$

* Electron Population Analysis of Accurate Diffraction Data. XII.
† Author to whom correspondence should be addressed.

0567-7394/83/030377-11$01.50

The cross terms $d_i d_j$ do not occur in the case of the isolated atom for which the electron density is diagonal in the orbitals. In the molecular case the cross terms only occur between orbitals belonging to the same symmetry representation which will occur together in a LCAO (linear combination of atomic orbitals) molecular orbital. Thus (1), in which all cross terms are represented, corresponds to the point-group symmetry $\bar{1}$.

In the case of $\bar{1}$ (C_i) all d orbitals transform according to the representation a_g and mixing is symmetry allowed. In more symmetric point groups mixing terms which violate the local symmetry do not occur. In the case of a square-planar point group ($4/mmm, D_{4h}$), for example, the d orbitals are of b_{1g}, a_{1g}, b_{2g} and e_g symmetry so that only the diagonal terms in (1) can occur. The corresponding density expression is

$$\rho_{3d} = P_1(d_{x^2-y^2})^2 + P_2(d_{z^2})^2 + P_3(d_{xy})^2 + \tfrac{1}{2}P_4(d_{xz}^2 + d_{yz}^2). \tag{2}$$

In trigonal point groups such as $3m(C_{3v})$ the atomic d orbitals split into a_{1g}, e_g and e_g' species (*e.g.* Ballhausen, 1962), of which e_g' correlates with the e_g orbitals of the octahedral point group. The electron-density expression for this symmetry includes a cross term between the components of the e_g orbitals:

$$\rho_{3d} = P_1 a_{1g}^2 + \tfrac{1}{2}P_2(e_{g+}^2 + e_{g-}^2) + \tfrac{1}{2}P_3(e_{g+}^{2\prime} + e_{g-}^{2\prime}) + \tfrac{1}{2}P_4(e_{g+}e_{g+}' + e_{g-}e_{g-}') \tag{3}$$

with $a_{1g} = d_{z^2}$, $e_{g+} = \sqrt{\frac{2}{3}}d_{x^2-y^2} - \sqrt{\frac{1}{3}}d_{xz}$; $e_{g-} = \sqrt{\frac{2}{3}}d_{xy} + \sqrt{\frac{1}{3}}d_{yz}$; $e_{g+}' = \sqrt{\frac{1}{3}}d_{x^2-y^2} + \sqrt{\frac{2}{3}}d_{xz}$ and $e_{g-}' = \sqrt{\frac{1}{3}}d_{xy} - \sqrt{\frac{2}{3}}d_{yz}$.

(*b*) *The electron density in terms of multipole density functions*

The electron density at each atom may be described by a spherical distribution, complemented with an expansion of multipole functions:

$$\rho(\mathbf{r}) = [\rho_{\text{core}}(r) + P_v\rho_{\text{valence}}(\kappa r) + \sum_{l=0}^{4}\left\{R_l(\kappa' r)\sum_{m=0}^{l}P_{lm\pm}y_{lm\pm}(\mathbf{r}/r)\right\}, \tag{4a}$$

where ρ_{core} and ρ_{valence} are spherical Hartree–Fock core and valence densities, the $y_{lm\pm}$ are the spherical harmonics in real form and R_l represents the radial part of the multipole functions. The second term in (4*a*) is a monopolar function with the radial distribution of the isolated-atom valence density for $\kappa = 1$. Expression (4*a*) is the basis for a least-squares procedure in which κ, κ', P_v and the P_{lm} are determined, together with the conventional structural parameters (Hansen & Coppens, 1978; Stewart, 1976).

For a transition-metal atom the d-electron density is described by the second and third terms in (4*a*):

$$\rho_d = P_v\rho_{\text{valence}}(\kappa r) + \sum_{l=0}^{4}\left\{R_l(\kappa' r)\sum_{m=0}^{l}P_{lm\pm}y_{lm\pm}(\mathbf{r}/r)\right\}. \tag{4b}$$

The equivalence of this expansion and (1) leads to relationships between the P_{lm} and the coefficients in (1) which are discussed in the following section.

(*c*) *Relation between atomic orbital coefficients and multipole population parameters*

Since the spherical harmonics are a complete set of functions, a product of two spherical harmonics is a linear combination of members of the set. In general the product $y_{lm\pm}y_{l'm'\pm}$ will contain terms with $l'' = |l - l'|$, $|l - l' + 2|\ldots, l + l'$ and with $m'' = |m - m'|_{\pm}$ and $|m + m'|_{\pm}$. Similar rules apply to products $y_{lm+}y_{l'm'-}$ except that $l'' = 0$ and $m'' = 0$ do not occur in this case. From coefficients available in the literature (Rose, 1957; Rae, 1978), (1) can be expressed as a sum of spherical harmonics in analogy to the multipole expansion (4).

Before the two expressions can be equated, however, the difference in normalization between the atomic orbitals ($\int y^2 d\tau = 1$) and the density functions ($\int |y| d\tau = 1$ for $l = 0$, $m = 0$, $\int |y| d\tau = 2$ for all higher multipoles) must be allowed for. When the different normalization factors (Hansen & Coppens, 1978) are taken into account, relations between the orbital coefficients P_i and the multiple populations $P_{lm\pm}$ are obtained which are represented by a matrix $\mathbf{M}$ defined by

$$\mathbf{P}_{lm\pm} = \mathbf{M}\mathbf{P}_i, \tag{5a}$$

where P_i is a 15-element vector of the coefficients of (1), $\mathbf{P}_{lm\pm}$ is a vector containing the coefficients of the 15 spherical-harmonic functions generated by the products of d orbitals, for which $l'' = 0$, 2 or 4.

The d-orbital occupancies can be derived from the experimental multipole populations by use of

$$\mathbf{P}_i = \mathbf{M}^{-1}\mathbf{P}_{lm\pm}. \tag{5b}$$

The inverse matrix $\mathbf{M}^{-1}$ given in Table 1 represents the generalized expression from which point-group-specific expressions can be derived by omission of symmetry-forbidden terms.

Point-group-specific expressions

The 'index picking' rules for the spherical harmonic functions under all crystallographic site symmetries have been given by Kurki-Suonio (1977). When combined with the condition $l = 0$, 2 or 4 nine different cases can be distinguished which are summarized in Table 2.

Table 1. *The matrix* $\mathbf{M}^{-1}$

d-orbital populations	Mutipole populations					
	P_{00}	P_{20}	P_{22}	P_{40}	P_{42}	P_{44}
P_{z^2}	0·200	1·04	0·00	1·40	0·00	0·00
P_{xz}	0·200	0·520	0·943	−0·931	1·11	0·00
P_{yz}	0·200	0·520	−0·943	−0·931	−1·11	0·00
$P_{x^2-y^2}$	0·200	−1·04	0·00	0·233	0·00	1·57
P_{xy}	0·200	−1·04	0·00	0·233	0·00	−1·57

Mixing terms

	P_{21}	P_{21-}	P_{22}	P_{22-}	P_{41}	P_{41-}	P_{42}	P_{42-}	P_{43}	P_{43-}	P_{44-}
$P_{z^2/xz}$	1·09	0·00	0·00	0·00	3·68	0·00	0·00	0·00	0·00	0·00	0·00
$P_{z^2/yz}$	0·00	1·09	0·00	0·00	0·00	3·68	0·00	0·00	0·00	0·00	0·00
P_{z^2/x^2-y^2}	0·00	0·00	−2·18	0·00	0·00	0·00	1·92	0·00	0·00	0·00	0·00
$P_{z^2/xy}$	0·00	0·00	0·00	−1·85	0·00	0·00	0·00	2·30	0·00	0·00	0·00
$P_{xz/yz}$	0·00	0·00	0·00	1·60	0·00	0·00	0·00	1·88	0·00	0·00	0·00
P_{xz/x^2-y^2}	1·88	0·00	0·00	0·00	−1·06	0·00	0·00	0·00	2·10	0·00	0·00
$P_{xz/xy}$	0·00	1·88	0·00	0·00	0·00	−1·06	0·00	0·00	0·00	2·10	0·00
P_{yz/x^2-y^2}	0·00	−1·88	0·00	0·00	0·00	1·06	0·00	0·00	0·00	2·10	0·00
$P_{zy/xy}$	1·88	0·00	0·00	0·00	−1·06	0·00	0·00	0·00	−2·10	0·00	0·00
$P_{x^2-y^2/xy}$	0·00	0·00	0·00	0·00	0·00	0·00	0·00	0·00	0·00	0·00	3·14

Table 2. *Allowed multipole functions describing d-orbital density*

	Point group	Allowed values of l, $m\pm$*	Dimension of **M**
I	1, $\bar{1}$	$l = 0, 2, 4$, all m	15 × 15
II	2, m, $2/m$	00, 20, 22+, 22−, 40, 42+, 42−, 44+, 44−	9 × 9
III	222, $m2m$, mmm	00, 20, 22+ 40, 42+, 44+	6 × 6
IV	4, $4/m$, $\bar{4}$	00, 20, 40, 44+, 44−	5 × 5 (4 × 4)†
V	422, $\bar{4}2m$, $4mm$, $4/mmm$	00, 20, 40, 44+	4 × 4
VI	3, $\bar{3}$	00, 20, 40, 43+, 43−	5 × 5 (4 × 4)†
VII	32, $3m$, $\bar{3}m$	00, 20, 40, 43+	4 × 4
VIII	6, $\bar{6}$, $6/m$, 622, $6mm$, $\bar{6}m2$, $6/mmm$	00, 20, 40	3 × 3
IX	23, $m3$, 432, $\bar{4}3m$, $m3m$	00, 40 + (0·7403)44+‡	2 × 2

* Principal symmetry axis is z axis.
† Dimension can be reduced by rotation of coordinate system, see text.
‡ This function is usually described as the cubic harmonic K_4.

In the triclinic point groups no further restrictions apply. Since y_{lm+} and y_{lm-} have φ dependences of cos $m\varphi$ and sin $m\varphi$ respectively, a vertical twofold axis limits m to either 2 or 4 in addition to the $m = 0$ values corresponding to cylindrically symmetric functions. For higher n-fold symmetry the only allowed functions with $m \neq 0$ are those with $m = n$. For sixfold symmetry this implies that only the cylindrically symmetric functions can result from electrons populating d orbitals.

Point groups with and without vertical mirror planes are distinguished by the occurrence of y_{lm-} functions in the latter case. This function may, however, be eliminated for $n = 3$ and $n = 4$ by a rotation of the coordinate system around the z axis, such as to change the zero of the φ angle, as shown by the following argument.

The φ dependence of the density is given by

$$\rho(\varphi) = P_{4n+} \cos n\varphi + P_{4n-} \sin n\varphi, \tag{6a}$$

which gives

$$\partial\rho/\partial\varphi = -nP_{4n+} \sin n\varphi + nP_{4n-} \cos n\varphi. \tag{6b}$$

Thus the maxima and minima occur at values of φ defined by

$$\tan n\varphi = P_{4n-}/P_{4n+}. \tag{7a}$$

A rotation of the coordinate system by

$$\varphi_0 = \frac{1}{n} \tan^{-1}(P_{4n-}/P_{4n+}) \tag{7b}$$

eliminates the antisymmetric component sin $n\varphi$, so that in this coordinate system the φ dependence may be written as

$$\rho(\varphi') = P'_{4n+} \cos n\varphi$$

with

$$P'_{4n+} = P_{4n+} \cos n\varphi_0 + P_{4n-} \sin n\varphi_0 \tag{8a}$$

or (equivalently)

$$P_{4n-} = P'_{4n+} \sin n\varphi_0$$
$$P_{4n+} = P'_{4n+} \cos n\varphi_0. \tag{8b}$$

When (7*b*) is applied, symmetries IV and V, and VI and VII of Table 2 become formally equivalent and the number of distinct cases is reduced to seven.

The matrix $\mathbf{M}^{-1}$ for specific point groups is obtained from Table 1 by elimination of *columns* corresponding to non-allowed multipoles. This leads to *rows* consisting only of zero's which represent non-symmetry-allowed cross terms in (1).

For example, for point group 2 (line II of Table 2) there are nine symmetry-allowed multipoles. The *d* orbitals in this point group belong to either the *a* (20, 22+, 22−) or the *b* (21+, 21−) representations. The density expression (1) then contains, in addition to the five diagonal terms, four cross terms (*i.e.* 20/22+, 20/22−, 22+/22−, 21+/21−). These nine terms correspond to the nine rows with at least one non-zero coefficient which are obtained when the symmetry-forbidden columns are deleted.

The 4 × 4 matrix for the square-planar case (row V of Table 2) is given in Table 3. The equality of the coefficients for P_{21+} and P_{21-} indicates the degeneracy of the d_{21+} and d_{21-} orbitals which belong to the e_g representation of D_{4h}. Thus $\frac{1}{2}P_4$ in (2) equals $P_{21+} = P_{21-}$.

The matrix for the trigonal point groups is listed in Table 4. The last column corresponds to the products of $d_{21+}d_{22-}$ and $d_{21-}d_{22+}$ which do not occur for the point groups 32, 3*m* and $\bar{3}m$. We note that these products also disappear when the zero of the azimuthal angle φ is shifted according to (8*b*).

Table 3. *Orbital–multipole relations for square-planar complexes* (*row* V *of Table* 2)

	Species in D_{4h}	P_{00}	P_{20}	P_{40}	P_{44+}
P_{20}	a_{1g}	0·200	1·039	1·396	0
P_{21+}	e_g	0·200	0·520	−0·931	0
P_{21-}		0·200	0·520	−0·931	0
P_{22+}	b_{1g}	0·200	−1·040	0·232	1·570
P_{22}	b_{2g}	0·200	−1·040	0·232	−1·570

Table 4. *Orbital–multipole relations for trigonal complexes* (*row* VI *of Table* 2)

	P_{00}	P_{20}	P_{40}	P_{43+}	P_{43-}
(*a*) In terms of *d* orbitals					
P_{20}	0·200	1·039	1·396	0	0
P_{21+}	0·200	0·520	−0·931	0	0
P_{21-}	0·200	0·520	−0·931	0	0
P_{22+}	0·200	−1·040	0·232	0	0
P_{22-}	0·200	−1·040	0·232	0	0
$P_{21+/22+}$	0	0	0	2·095	0
$P_{21+/22-}$	0	0	0	0	2·095
$P_{21-/22+}$	0	0	0	0	2·095
$P_{21-/22-}$	0	0	0	−2·095	0
(*b*) In terms of symmetry-adapted orbitals (expression 3)*					
$P_1\,(a_{1g})$	0·200	1·040	1·396	0	
$P_2\,(e_g)$	0·400	−1·040	−0·310	−1·975	
$P_3\,(e'_g)$	0·400	0	−1·087	1·975	
$P_4(e_{g+}e'_{g+} + e_{g-}e'_{g-})$	0	−2·942	2·193	1·397	

* The signs given here imply a positive e'_g lobe in the positive *xz* quadrant. Care should be exercised in defining the coordinate system if this lobe is to point towards a ligand atom.

Application of the expressions

The expressions described above have been applied to a series of transition-metal complexes. Some representative examples, summarized in Table 5, are given here. They include four metal–carbonyl complexes of varying symmetry and the complex ionic solid hexaamminecobalt(III) hexacyanocobaltate(III), which was among the first transition-metal complexes of which the experimental density was determined by X-ray diffraction techniques (Iwata & Saito, 1973).

Crystallographic and local site symmetries are listed in columns 4 and 5 of Table 5. Since preliminary refinements invariably indicated that multipoles not allowed by the local symmetry at the transition-metal site are not significantly populated, a local symmetry constraint was imposed in all refinements reported here.

In all cases the weight $w(F^2)$ equalled $1/\sigma^2(F^2)$ with $\sigma^2(F^2) = [\sigma^2_{\text{count}} + (CF^2)^2]^{1/2}$ with $C = 0{\cdot}02$ and $C = 0{\cdot}01$ for the metal-carbonyl complexes and for the hexaammine cobalt salts respectively. Since parameters for the 4*s* electrons can often not be refined because of the limited influence of 4*s* scattering on the diffraction intensities, several refinements were done with and without the inclusion of 4*s* electrons. All core- and isolated-atom valence scattering factors were taken from *International Tables for X-ray Crystallography* (1974). Scattering factors for the 4*s* electrons were as calculated by Cromer (1977).

In addition all transition-metal carbonyl complexes reported here were analyzed with two different radial functions for the monopolar term, corresponding respectively to an isolated-atom Hartree–Fock 3*d* radial function modified by κ, (the second term in 4*a*) and a Slater-type radial function with the same radial dependence as the higher multipoles (the monopole of the third term in 4*a*). Since the resulting population parameters are very similar only results of the first treatment, which gave slightly lower *R* factors, are

Table 5. *Summary of examples*

Compound	Space group	*Z*	Site symmetry: Crystallographic	Site symmetry: Local (assumed)	Reference to data set
$Cr(CO)_6$	*Pnma*	4	*m*	4/*m* 3*m*	Rees & Mitschler (1976)
$Mn_2(CO)_{10}$	*I*2/*a*	4	1	4 *mm*	Martin, Rees & Mitschler (1982)
$Co_2(CO)_8$	$P2_1/m$	4	1	*m*	Leung & Coppens (1983)
$Co_3(CO)_9CH$	$P\bar{1}$	2	1	*m*	Leung & Coppens (1983)
$Co(NH_3)_6Cr(CN)_6$	$R\bar{3}$	1	$\bar{3}$	$\bar{3}$	Iwata (1977)
$Co(NH_3)_6Co(CN)_6$	$R\bar{3}$	1	$\bar{3}$	$\bar{3}$	Iwata & Saito (1973)

Table 6. *Summary of refinements, population parameters and κ and ζ values*

(*a*) Summary of refinements

	Temperature (K)	Number of observations	$(\sin\theta/\lambda)_{max}$ (Å^{-1})	Free-atom refinement				κ refinement				Multipole refinement with 4*s*			Multipole refinement without 4*s*			
				R†	R_w	S	NV	R	R_w	S	NV	R	R_w	S	R	R_w	S	NV
$Cr(CO)_6$*	74	2915	1·08	4·27	6·93	1·64	68	4·23	6·38	1·51	74	3·21	5·05	1·20	3·19	5·03	1·19	85
$Mn_2(CO)_{10}$*	74	1991	0·76	2·81	5·05	1·53	100	—	—	—	—	2·29	3·43	1·04	2·17	3·37	1·03	120
		4696	1·32									4·02	5·51	1·16	3·94	5·39	1·19	120
$Co_2(CO)_8$*	100	5346	1·04	4·30	7·43	1·39	175	—	—	—	—	3·83	6·54	1·23	4·10	6·61	1·24	220
$Co_3(CO)_9CH$*	100	8046	1·20	4·85	6·40	2·03	203	4·88	6·25	1·99	212	4·48	5·61	1·80	4·61	5·76	1·83	238
$Co(NH_3)_6Cr(CN)_6$	80	2042	1·08	2·96	3·34	2·50	35	—	—	—	—	—	—	—	2·04	2·19	1·65	68
$Co(NH_3)_6Co(CN)_6$	300	2047	1·27	3·09	3·76	1·84	35	—	—	—	—	—	—	—	2·31	2·74	1·33	68

(*b*) Least-squares population parameters for the transition-metal elements

	P_{00}	P_{11+} / P_{11-}	P_{10}	P_{20}	P_{21+} / P_{21-}	P_{22}	P_{30}	P_{31+} / P_{31-}	P_{32+} / P_{32-}	P_{33+} / P_{33-}	P_{40}	P_{41+} / P_{41-}	P_{42}	P_{43+} / P_{43-}	P_{44}
$Cr(CO)_6$	4·69 (9)	—	—	—	—	—	—	—	—	—	0·18 (2)	—	—	—	0·12
$Mn_2(CO)_{10}$	5·82 (3)	—	0·03 (2)	0·04 (1)	—	—	0·01 (1)	—	—	—	0·26 (2)	—	—	—	0·20 (3)
$Co_2(CO_8$‡	7·70 (3)	0·14 (2)	0·05 (1)	0·07 (1)	0·02 (1)	0·05 (1)	0·02 (1)	0·06 (1)	0·02 (1)	0·00 (1)	0·04 (2)	0·02 (1)	0·03 (1)	0·11 (2)	0·01 (2)
$Co(CO)_9CH$§	7·26 (2)	0·03 (2)	0·11 (1)	0·02 (1)	0·02 (1)	0·12 (1)	0·02 (2)	0·01 (2)	0·01 (2)	0·01 (2)	0·12 (3)	0·15 (2)	0·19 (3)	0·04 (3)	0·15 (3)
$Co(NH_3)_6Cr(CN)_6$															
Co	7·84 (9)	—	—	0·20 (4)	—	—	—	—	—	—	0·51 (4)	—	—	0·35 (4)	—
														0·04 (4)	
Cr	5·36 (9)	—	—	0·20 (4)	—	—	—	—	—	—	0·13 (4)	—	—	0·18 (4)	—
														0·01 (4)	
$Co(NH_3)_6Co(CN)_6$															
$Co(NH_3)$	7·44 (9)	—	—	0·02 (6)	—	—	—	—	—	—	0·21 (7)	—	—	0·51 (6)	—
														0·08 (6)	
$Co(CN)$	7·26 (9)	—	—	0·06 (7)	—	—	—	—	—	—	0·30 (7)	—	—	0·36 (6)	—
														0·06 (7)	

(*c*) κ and ζ values¶**

	κ	ζ (a.u.$^{-1}$)	Theoretical ζ†† neutral atom (a.u.$^{-1}$)
$Cr(CO)_6$	0·99 (2)	6·8 (7)	6·5
$Mn_2(CO)_{10}$ (all data)	0·998 (10)	8·0 (5)	7·0
$Co_2(CO)_8$	1·017 (8)	6·9 (2)	7·9
$Co_3(CO)_9CH$	1·112 (6)	10·0 (3)	7·9
$Co(NH_3)_6Cr(CN)_6$			
$Co(NH_3)_6$	1·037 (3)	9·2 (4)	7·9
$Cr(CN)_6$	1·113 (7)	8·0 (5)	6·5
$Co(NH_3)_6Co(CN)_6$			
$Co(NH_3)_6$	1·007 (3)	5·7 (4)	7·9
$Co(CN)_6$	1·022 (4)	8·8 (8)	7·9

* All CO groups assumed equivalent.

† R factors defined as $\sum ||Y_{obs} - kY_{calc}|| / Y_{obs}$ and $R_w = [\sum w(Y^2_{obs} - k^2 Y^2_{calc})^2 / \sum w Y^4_{obs}]^{1/2}$, with $Y = F^2$ for the first four compounds and $Y = F$ for last two entries in the Table.

‡ x axis in mirror plane, $lm+$ allowed for m odd.

§ x axis perpendicular to mirror plane, $lm-$ allowed for m odd.

¶ From refinements without 4*s* functions.

** κ as defined in (4*a*); ζ is defined by $R_l = r^4 \exp(-\zeta r)$.

†† Clementi & Raimondi (1963).

listed in the tables. R factors are compared with those from the free-atom and the spherical-atom κ refinements (Coppens, Guru Row, Leung, Stevens, Becker & Yang, 1979) in Table 6*a*. A considerable improvement in R factors and in goodness of fit S is observed for all refinements. The improvement on introducing atomic asphericity (*i.e.* the difference between the κ and multipole refinement results) is larger than the decrease in R and S on introduction of ionicity and valence-shell expansion and contraction (*i.e.* the difference between the free-atom and the κ refinement). Though this is not surprising given the larger increase in number of parameters in the former case, it contrasts with our experience with light-atom-only molecules for which the largest improvement is often obtained on the introduction of charge transfer between atoms.

Transition-metal population parameters and κ and ζ values from the multipole refinements are listed in Tables 6*b* and *c*. Coordinate systems are defined in Fig. 1.

A brief description of the results for each of the compounds follows.

$Cr(CO)_6$

Chromium hexacarbonyl is an octahedral complex for which a careful electron density study has been reported by Rees & Mitschler (1976). A self-consistent field calculation with the $X\alpha$ exchange approximation has been described by Heijser (1979).

Only two multipoles are allowed for the octahedral local symmetry. They are y_{00}, and the cubic harmonic $y_{40} + 0{\cdot}7403y_{44+}$. Separate refinement of P_{40} and P_{44+}, which is possible in this case because of the lower crystallographic symmetry, gave a ratio very close to that required in the octahedral field.

Results listed in Table 7 are almost independent of the treatment of the 4*s* electron, indicating that the asphericity is a much better defined property than the net charge, which is ambiguous because of the diffuseness of the 4*s* distribution. Here and in the other compounds studied orbital occupancies are in very reasonable agreement with theoretical values and deviate appreciably from the spherical-atom configuration.

A dynamic model map calculated with Fourier coefficients

$$(F_{\text{calc, multipole model}} - F_{\text{calc, spherical-atom model}})$$

is shown in Fig. 2(*a*). The errors in the multipole model maps may be judged from the residual maps, based on

$$F_{\text{obs}} - F_{\text{calc, multipole model}},$$

which are a measure of the fit of the model to the experimental density distribution. Residual maps have been calculated for all the refinements reported here. In the case of $Cr(CO)_6$ the map reproduced in Fig. 2(*b*) indicates that a good-quality fit has been obtained.

$Mn_2(CO)_{10}$

Dimanganese decacarbonyl was studied by Martin, Rees & Mitschler (1982). Though the main aim of the study was elucidation of the nature of the metal–metal bonding, the data also contain information on the charge asphericity around the metal atom. Results of the multipole refinements are listed in Table 8. Comparison of the low-order with all-data refinement shows good agreement between the two sets of results. This suggests that *d*-orbital occupancies can be derived even when high-order data are not available. Relative to the spherical atom the a_1 and b_2 orbitals which point toward the ligands are destabilized, the effect being

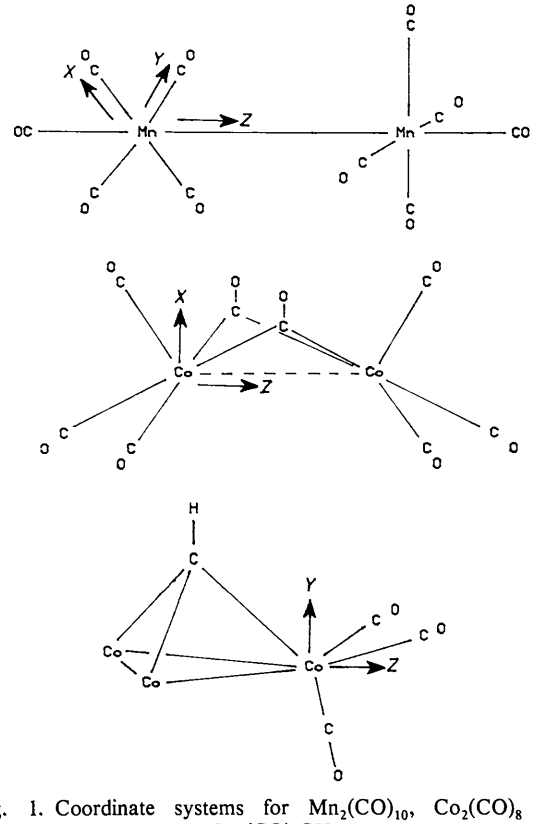

Fig. 1. Coordinate systems for $Mn_2(CO)_{10}$, $Co_2(CO)_8$ and $Co_3(CO)_9CH$.

Table 7. *Orbital populations for* $Cr(CO)_6$

	With 4*s*	Without 4*s*	Theoretical	Spherical atom
e_g	1·42 (5)	1·37 (7)	1·12	2
t_{2g}	3·40 (5)	3·32 (8)	3·26	3
Total *d*	4·82 (9)	4·69 (9)	4·38	5
4*s*	1	—	−0·085	1
$4p_x$			−0·011	
$4p_y$			−0·011	
$4p_z$			−0·011	

smaller for a_1 which has one CO and one Mn neighbor. Agreement with theory is satisfactory, though the destabilization is somewhat more pronounced than predicted by the theory.

The model map (shown in Fig. 3*a*) contains both the plane through the metal atom and three carbonyl groups, and the plane bisecting the equatorial carbonyl ligands, because the two metal carbonyl groups are

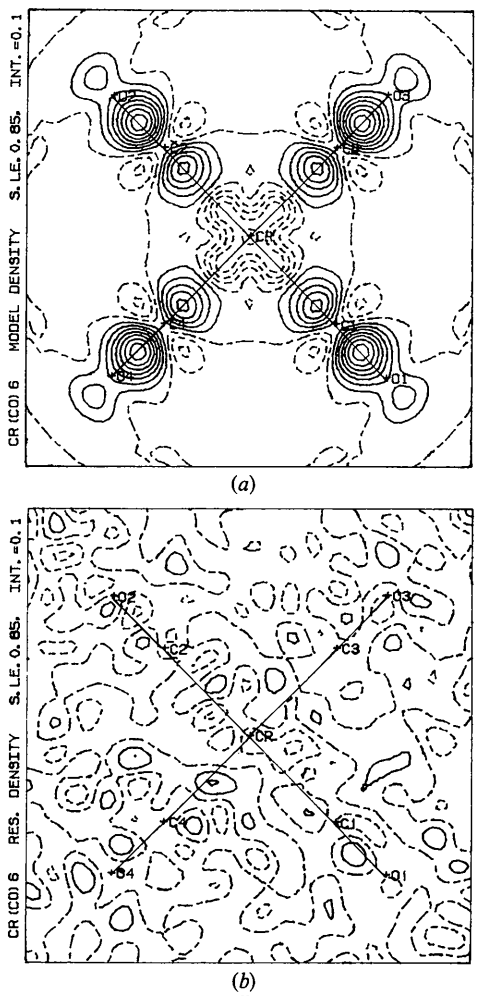

Fig. 2. $Cr(CO)_6$. Refinement without 4*s* orbitals. Contours at 0·1 e Å^{-3}, zero and negative contours broken; sin $\theta/\lambda < 0{\cdot}85$ Å^{-1}. (*a*) Model density in a plane containing $Cr(CO)_4$. (*b*) Residual density.

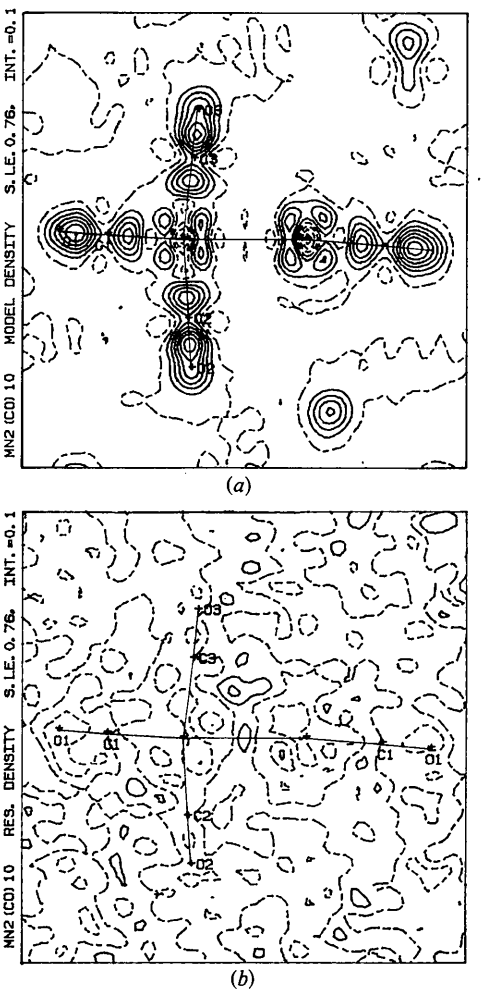

Fig. 3. $Mn_2(CO)_{10}$. Refinement without 4*s* orbitals. Data with sin $\theta/\lambda < 0{\cdot}76$ Å^{-1}. Contours as in Fig. 2. (*a*) Model density in a plane containing two Mn atoms and four carbonyl groups. (*b*) Residual density in one of the chemically equivalent planes.

Table 8. *Orbital populations for* $Mn_2(CO)_{10}$

See Fig. 1 for definition of the coordinate system.

	Low-order data (sin $\theta/\lambda < 0{\cdot}76$ Å^{-1})		All data (sin $\theta/\lambda < 1{\cdot}32$ Å^{-1})					
	With 4*s*	Without 4*s*	With 4*s*		Without 4*s*		Theoretical		Spherical atom	
a_1 (d_{z^2})	0·67 (3)	0·80 (3)	0·76 (3)	14·2%	0·84 (3)	14·2%	0·85	16·1%	1·0	20%
b_2 ($d_{x^2-y^2}$)	0·59 (4)	0·70 (4)	0·65 (4)	12·1%	0·76 (4)	13·0%	1·81	34·3%	2·0	40%
b_1 (d_{xy})	1·19 (4)	1·31 (4)	1·27 (4)	23·6%	1·37 (4)	23·5%				
e (d_{xz}, d_{yz})	2·51 (4)	2·80 (4)	2·69 (3)	50·1%	2·86 (3)	49·1%	2·61	49·5%	2·0	40%
Total *d*	4·95 (3)	5·60 (3)	5·37 (3)		5·83 (3)		5·27		5·0	
4*s*	2	—	2		—		−0·24			
$4p_x$							−0·12			
$4p_y$							−0·12			
$4p_z$							0·24			

symmetry related in a staggered conformation. The accumulation of *d*-orbital lone-pair density near the metal atoms is evident. The corresponding residual map (Fig. 3*b*) is almost featureless.

$Co_2(CO)_8$

Dicobalt octacarbonyl is a doubly bridged dinuclear species, the structure of which was first studied by Sumner, Klug & Alexander (1964). The electron-density analysis of $Co_2(CO)_8$, based on a new set of data collected at 100 K, will be described in detail in a separate publication. The populations of the *d* orbitals obtained from the multipole refinement are listed in Table 9. The agreement with the theoretical results of Heijser is again quite close, except for the d_{xz} orbital which is slightly depopulated relative to the spherical d^7 configuration according to the experiment, and has some excess density according to the theory.

Model maps through two terminal carbonyls and the cobalt atoms, through the bridging ligand containing both cobalts, and through the bridging ligand perpendicular to the Co–Co vector, are shown in Figs. 4(*a*), (*c*) and (*d*) respectively. The lone pair at the bridging CO carbon atom is not cylindrically sym-

Table 9. *Orbital populations for* $Co_2(CO)_8$

See Fig. 1 for definition of coordinate system.

	Experimental					
	With 4*s*		Without 4*s*		Theoretical	
d_{z^2}	1·57 (4)	22·0%	1·67 (4)	21·7%	1·53	21·2%
$d_{x^2-y^2}$	1·53 (4)	21·5%	1·61 (3)	20·9%	1·49	20·7%
d_{xy}	1·34 (4)	18·8%	1·46 (3)	19·0%	1·31	18·4%
d_{xz}	1·36 (3)	19·1%	1·50 (3)	19·5%	1·55	21·5%
d_{yz}	1·31 (3)	18·4%	1·46 (3)	19·0%	1·33	18·4%
Total *d*	7·11 (3)		7·70 (3)		7·21	
4*s*	2		0		−0·02	
$4p_x$					0·16	
$4p_y$					0·04	
$4p_z$					0·35	

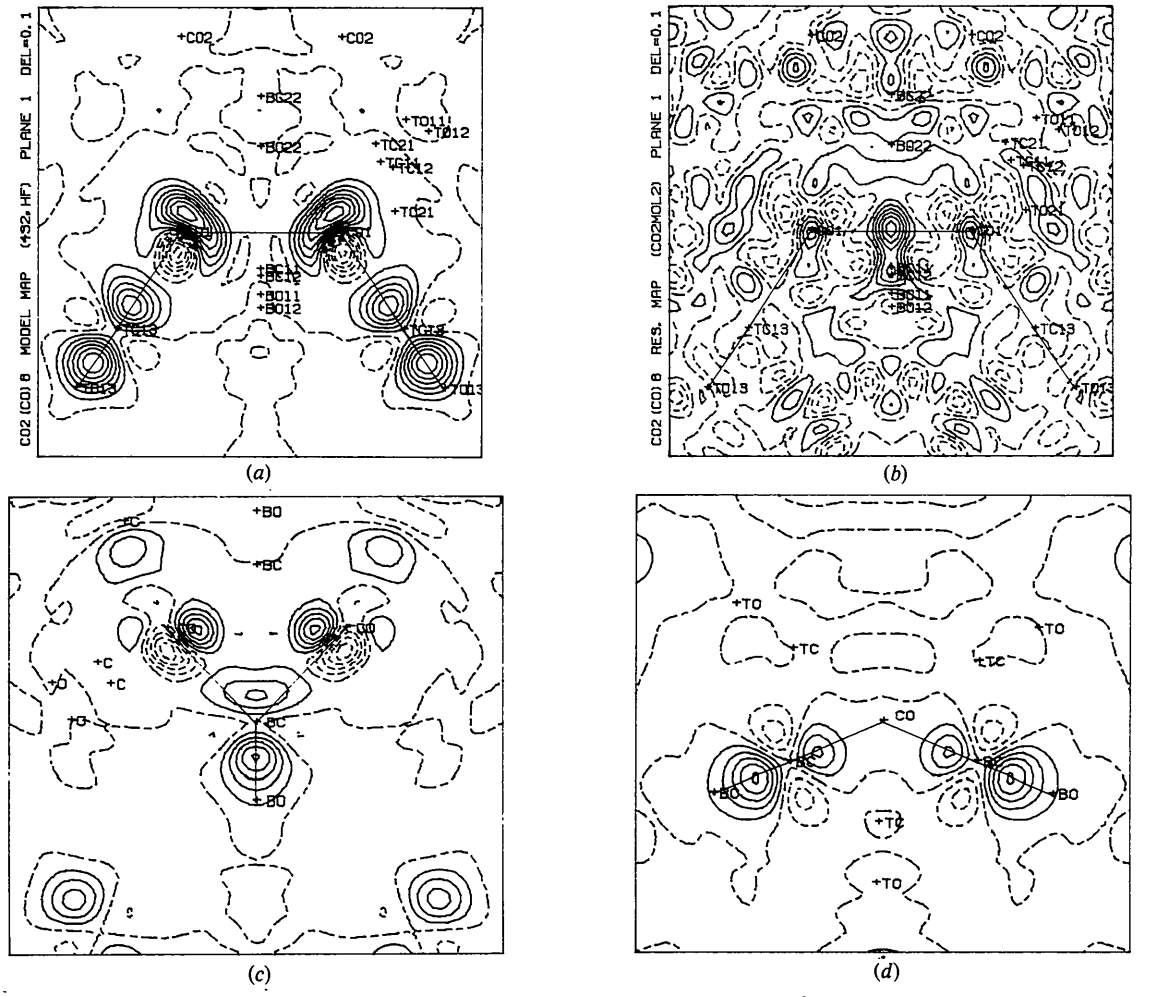

Fig. 4. $Co_2(CO)_8$. Refinement including 4*s* orbitals. Contours as in Fig. 2, $\sin\theta/\lambda < 0{\cdot}85$ Å^{-1}. (*a*) Model density in a plane containing two Co atoms and two terminal carbonyl groups. (*b*) Residual density in one of the chemically equivalent planes corresponding to (*a*). (*c*) Model density in a plane containing the bridging carbonyl and two Co atoms. (*d*) Model density in the plane containing the bridging carbonyl perpendicular to the Co–Co vector.

metric, as it would be in the isolated carbon monoxide molecule, but considerably extended in the plane of the metal atoms due to metal–ligand bonding. Fig. 4(*a*) shows a polarization of the 3*d* density towards the position of the 'missing' bridging CO group.

The residual map corresponding to Fig. 4(*a*) (Fig. 4*b*) shows an accumulation of density at Co–Co bond midpoint which cannot be accounted for by the atom-centered multipole functions. The map is generally noisier than those of the two compounds discussed previously; this is probably a result of a difference in data quality between the two sets.

$Co_3(CO)_9CH$

Nonacarbonylmethylidynetricobalt was studied as part of our program concerning the charge distribution in metal cluster compounds. The results of the neutron diffraction analysis have been reported previously (Leung, Coppens, McMullan & Koetzle, 1981). The theoretical calculation performed on this much larger molecule is based on the approximate non-empirical Fenske–Hall method (Ortega, 1980). Though the general trend in the relative population of the metal *d* orbitals is the same in theory and experiment (Table 10), fairly large numerical differences are observed, which may be at least partially attributed to the more approximate nature of the calculation for this compound.

Model and residual densities in one of the CoCHCO planes are shown in Fig. 5.

$Co(NH_3)_6Cr(CN)_6$ *and* $Co(NH_3)_6Co(CN)_6$

Electron-density studies of the coordination complexes hexaamminecobalt(III) hexacyanocobaltate(III) and hexaamminecobalt(III) hexacyanochromate(III) were reported in 1973 (Iwata & Saito, 1973) and 1977 (Iwata, 1977). Though a partial population analysis was described in the second publication, the large

Table 10 *Orbital populations for* $Co_3(CO)_9CH$

See Fig. 1 for definition of coordinate system.

Orbital	Experimental		Theoretical (Fenske–Hall)
	With 4*s*	Without 4*s*	
d_{z^2}	1·43 (5)	1·50 (4)	1·65
$d_{x^2-y^2}$	1·26 (5)	1·37 (4)	1·50
d_{xy}	1·77 (5)	1·83 (4)	1·69
d_{xz}	0·80 (5)	0·96 (5)	1·17
d_{yz}	1·60 (5)	1·61 (5)	1·61
Total 3*d*	6·85 (2)	7·26 (3)	7·62
4*s*	2	—	0·49
$4p_x$	—	—	0·51
$4p_y$	—	—	0·61
$4p_z$	—	—	0·40
	2·00		2·01

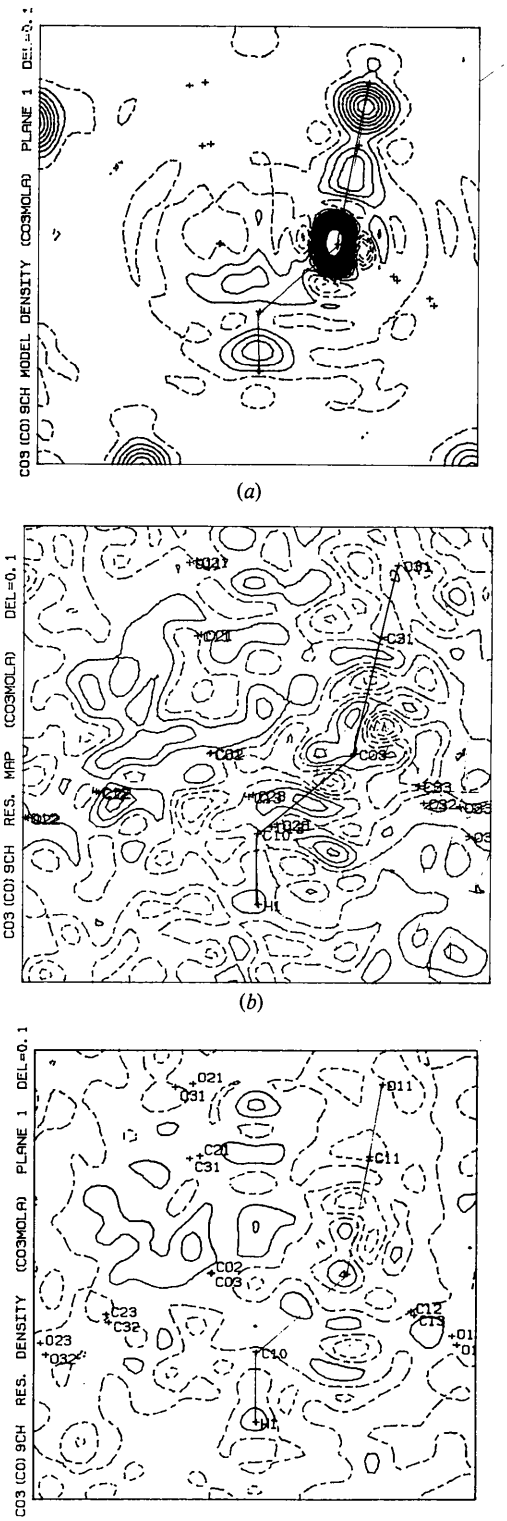

Fig. 5. $Co_3(CO)_9CH$. Refinement including 4*s* orbitals. Contours as in Fig. 2, $\sin\theta/\lambda < 0{\cdot}85$ Å^{-1}. (*a*) Model density in a plane containing a Co atom, a CO and the CH ligand. (*b*) Residual density in one of the corresponding chemically equivalent planes. (*c*) Residual density averaged over three chemically equivalent planes.

Table 11. *Comparison of orbital populations of* $Co(NH_3)_6Cr(CN)_6$, $Co(NH_3)_6Co(CN)_6$ *and* $Cr(CO)_6$

From treatment with zero 4*s* population.

	Spherical atom	$Co(NH_3)_6^{3+}$	$Cr(CN)_6^{3-}$	$CO(NH_3)_6^{3+}$	$Co(CN)_6^{3-}$	$Cr(CO)_6$
a_g (%)	20	26·4	19·4	24·3	25·0	70·8
e_g (%)	40	49·6	49·9	52·2	49·2	
e_g' (%)	40	24·1	30·7	23·5	25·9	29·2
Total 3*d* population		7·84	5·26	7·44	7·26	4·69

reported populations of the e_g' orbitals which point towards the ligands seem to contradict the deformation density maps which show accumulations in the e_g directions.

The results of the *d*-orbital analysis (Table 11) indicate preferential occupancy of the e_g and a_g orbitals of the slightly distorted octahedral complexes, in agreement with the deformation densities. In all cases the e_g' orbital is depopulated relative to the spherical atom. The remaining non-zero population of e_g' is an indication of covalent metal–ligand interaction in these low-spin complexes, which is larger for the cyano ligand than for the ammonia molecule, in agreement with accepted chemical concepts (*e.g.* Cotton & Wilkinson, 1972).

The agreement between the two hexaammine cations is satisfying, especially in view of the fact that the earlier study was performed at room temperature. Very little difference is observed between the relative orbital occupancies of the $Cr(CN)_6^{3-}$ ion and the $Cr(CO)_6$ molecule (last column of Table 11) indicating a close similarity between the isoelectronic CN^- and CO ligands. Both agreements support the reproducibility of the results.

Discussion

The reproducibility of the *d*-orbital occupancies as reported in Table 11, and the agreement between experimental and theoretical populations shown in Tables 7–10, support the validity of the methods used. Further work is needed to analyze the significance of remaining discrepancies. The insensitivity of the results to the inclusion of 4*s* electrons in the refinement formalism indicates the indeterminacy of the total transition-metal electron population. The 4*s* electrons have a diffuse distribution which peaks near neighboring ligand atoms. The scattering of these electrons can be accounted for about equally well by ligand-atom-centered functions. A similar ambiguity exists in direct-space partitioning techniques. When the total density is partitioned using boundaries perpendicular to the interatomic vectors the 4*s* density of, for example, the cobalt atom in $Co_3CH(CO)_9$, is invariably apportioned to the ligand atoms (Holladay & Coppens, 1983). On the other hand, partitioning of the deformation density implies *a priori* assignment of the 4*s* density to the transition-metal atom. The choice is arbitrary and the ambiguity analogous to that occurring in the least-squares treatment. The *d* orbital occupancies on the other hand are derived from the angular dependence of the transition-metal density which is much better defined, both in experiment and theory. The observed agreement is to be interpreted as an agreement in the angular functions. The radial dependence of the functions used is generally not the same in theory and experiment, and dependent on the choice of basis set.

The analysis given here does not consider the cross terms in (1), which are symmetry allowed for $Co_2(CO)_9$ and $Co_3CH(CO)_9$. The cross terms integrate to zero and therefore do not contribute to net populations even though they constitute an integral part of the description of the electron distribution. The cross terms are not listed when theoretical population analyses are reported, so that a comparison is not possible at present.

κ and ζ values for refinements excluding 4*s* orbitals are listed in Table 6*c*. The most pronounced deviation from isolated atom values is observed for the tricobalt cluster $Co_3(CO)_9CH$ in which cobalt valence shells are considerably contracted. Interpretation of the possible significance of this result is premature and requires similar analysis of other cluster compounds.

Conclusion

The analysis developed above allows the determination of *d*-orbital occupancies of transition-metal atoms. It is especially helpful for complexes of which the electronic ground state has not been established unambiguously. Applications to such systems are in progress and will be reported in subsequent publications.

The authors would like to thank Professor E. D. Stevens for helpful discussions and Dr D. T. Cromer for providing the 4*s* scattering factors. Support of this work by the National Science Foundation (CHE 7905897) is gratefully acknowledged.

References

BALLHAUSEN, C. (1962). *Introduction to Ligand Field Theory*. New York: McGraw-Hill.

BENARD, M., COPPENS, P., DELUCIA, M. L. & STEVENS, E. D. (1980). *Inorg. Chem.* **19**, 1924–1930.

CLEMENTI, E. & RAIMONDI, D. L. (1963). *J. Chem. Phys.* **38**, 2686–2689.
COPPENS, P., GURU ROW, T. N., LEUNG, P., STEVENS, E. D., BECKER, P. J. & YANG, Y. W. (1979). *Acta Cryst.* A**35**, 63–72.
COTTON, F. A. & WILKINSON, G. (1972). *Advanced Inorganic Chemistry*, 3rd ed. New York: Wiley.
CROMER, D. T. (1977). Private communication.
DOWNS, J. W., HILL, R. J., NEWTON, M. D., TOSSELL, J. A. & GIBBS, G. V. (1982). In *Electron Distributions and the Chemical Bond*, edited by P. COPPENS & M. B. HALL. New York: Plenum.
HANSEN, N. K. & COPPENS, P. (1978) *Acta Cryst.* A**34**, 909–921.
HEIJSER, W (1979). PhD Thesis. Free Univ., Amsterdam, Holland.
HOLLADAY, A. & COPPENS, P. (1983). In preparation.
International Tables for X-ray Crystallography (1974). Vol. IV. Birmingham: Kynoch Press.
IWATA, M. (1977). *Acta Cryst.* B**33**, 59–69.
IWATA, M. & SAITO, Y. (1973). *Acta Cryst.* B**29**, 822–832.
KURKI-SUONIO, K. (1977). *Isr. J. Chem.* **16**, 115–123.
LEUNG, P. & COPPENS, P. (1983). In preparation.
LEUNG, P., COPPENS, P., MCMULLAN, R. K. & KOETZLE, T. F. (1981). *Acta Cryst.* B**37**, 1347–1352.
MARTIN, M., REES, B. & MITSCHLER, A. (1982). *Acta Cryst.* B**38**, 6–15.
MOSS, G., HANSEN, N. K. & COPPENS, P. (1980). In *Computing in Crytallography*, edited by R. DIAMOND, S. RAMASESHAN & K. VENKATESAN. Bangalore: Indian Academy of Sciences.
ORTEGA, R. B. (1980). PhD Thesis. Univ. of New Mexico.
RAE, A. D. (1978). *Acta Cryst.* A**34**, 719–724.
REES, B. & COPPENS, P. (1973). *Acta Cryst.* B**29**, 2516–2528.
REES, B. & MITSCHLER, A. (1976). *J. Am. Chem. Soc.* **98**, 7918–7924.
ROSE, M. E. (1957). *Elementary Theory of Angular Momentum*. New York: Wiley.
STEVENS, E. D. & COPPENS, P. (1979). *Acta Cryst.* A**35**, 536–539.
STEWART, R. F. (1972). *J. Chem. Phys.* **57**, 1664–1668.
STEWART, R. F. (1976). *Acta Cryst.* A**32**, 565–574.
STEWART, R. F. (1977). *Chem. Phys. Lett.* **49**, 281–284.
SUMNER, G. G., KLUG, H. P. & ALEXANDER, L. E. (1964). *Acta Cryst.* **17**, 732–742.
WANG, Y. W. & COPPENS, P. (1976). *Inorg. Chem.* **15**, 1122–1127.
WEISS, R. J. & MAZZONE, G. (1981). *J. Appl. Cryst.* **14**, 401–416.

Acta Cryst. (1983). A**39**, 387–399

Dynamical X-ray Propagation: a Theoretical Approach to the Creation of New Wave Fields

BY F. BALIBAR

Laboratoire de Minéralogie–Cristallographie, associé au CNRS, Université Pierre et Marie Curie (Paris 6) et Paris 7, 4 place Jussieu, 75230 Paris CEDEX 05, France

F. N. CHUKHOVSKII

Institute of Crystallography, Academy of Sciences of the USSR, Moscow, USSR

AND C. MALGRANGE

Laboratoire de Minéralogie–Cristallographie, associé au CNRS, Université Pierre et Marie Curie (Paris 6) et Paris 7, 4 place Jussieu, 75230 Paris CEDEX 05, France

(*Received* 24 *February* 1982; *accepted* 2 *December* 1982)

Abstract

Although it is commonly invoked, the phenomenon of 'creation of new wave fields', which is responsible for some of the features visible on topographic images, has never been really explained in theoretical terms. This is done here in the case of a crystal deformed by a uniform strain gradient. The appropriate Green function is expanded in reciprocal space as a wave packet of non-plane waves, each component corresponding to a single value of the deviation parameter at the entrance surface. It is then shown that each component of this wave packet is made up of four parts, two of which can be identified as 'normal' wave fields (*i.e.* those predicted by the Eikonal theory); the two others are the so-called 'created wave fields'; it is shown that they correspond to interbranch scattering from one branch of the dispersion surface to the other and give rise to two extra beams. These created wave fields extract a fraction $e^{-2\pi|v|}$ out of the normal energy flow ($|v|$ being inversely proportional to the strain gradient), in full agreement with previous computer experiments.

I. Introduction

Understanding the so-called 'creation of new wave fields' in highly distorted parts of a crystal has been one

0567-7394/83/030387-13$01.50